Design parameter evaluation of a metal recoated Fiber Bragg Grating sensors for measurement of cryogenic temperature or stress in superconducting devices

R. Rajinikumar [a,b,c,*], M. Süßer [a], K.G. Narayankhedkar [d], G. Krieg [c], M.D. Atrey [b]

[a] Institute of Technical Physics, Forschungszentrum Karlsruhe, P.O. Box 3640, D-76021 Karlsruhe, Germany
[b] Department of Mechanical Engineering, Indian Institute of Technology Bombay, 400 076 Mumbai, India
[c] Sensor System Technology, University of Applied Sciences, P.O. Box 2440, D-76012 Karlsruhe, Germany
[d] Veermata Jijabai Technological Institute, 400 019 Mumbai, India

ARTICLE INFO

ABSTRACT

There are plenty of complex physical phenomena which remain to be studied and verified experimentally for building an optimized superconducting magnet. The main problem for experimental validations is due to the unavailability of suitable sensors. This paper proposes a Fiber Bragg Gratings (FBG) sensor for this purpose which allows access to the local temperature/stress state. To measure the low temperature (20 K), FBG can be recoated with materials having high thermal expansion coefficient (HTCE). This can induce a thermal stress for a temperature change, which in turn increases the sensitivity of the sensor. The performance of such sensors has been experimentally studied and reported in earlier paper [Rajinikumar R, Suesser M, Narayankhedkar KG, Krieg G, Atrey MD. Performance evaluation of metallic coated Fiber Bragg Grating sensors for sensing cryogenic temperature. Cryogenics 2008;48:142–7]. This paper aims at evaluation and determination of different design parameters like coating materials, coating thickness, grating period and the grating length for design of better performance FBG sensor for low temperature/stress measurements.

1. Introduction

The ability to provide real time information for super conducting (SC) magnets is an important diagnostic process for effective design, construction and protection of the SC magnet. There are many parameters like current density, magnetic flux, critical temperature, stress, define an optimised SC magnet design. Knowing the temperature and stress distribution inside the SC magnets at specific location could help the magnet designer to identify the exact location of the hotspot generated and the direction of the propagation of the hotspot. The stability margin, the hot spot temperature, the maximum pressure in Cable in Conduit Conductors (CICC), the helium explosion from the CICC cables and the hoop and thermal stress distributions in the conductor cross-section are a few problems worth to be investigated in more detail. Based on this information, the magnet designer can improve the design by modifying the material, routing the cooling channel in the required place and so on. A considerable theoretical effort was dedicated to the understanding of the complex physical properties associated with SC magnets but the experimental validation is missing. The main problem for experimental validations is due to the unavailability of the suitable sensors. Electrical strain gauge (ESG), diodes and many other conventional electro-mechanical sensor systems are considered. Unfortunately, these sensors are susceptible to the electromagnetic interference (EMI). In addition, the number of sensors required for long SC cables will be more to get the signal distribution. Also, the risk involved in introducing electrical wires inside the SC magnets makes them unsuitable candidate for the needed measurement system. Use of FBG sensors is very appealing for sensing the low temperature and stress in super conducting magnets because of their miniature size and the possibility of having many sensors in single fiber.

Even though the FBG sensors are more suitable candidate to study the above mentioned phenomena, the main drawback of these sensors are their low intrinsic thermal sensitivity at low temperatures. This is due to very low thermal expansion coefficient of glass fiber around ∼120 K. In fact, the intrinsic temperature sensitivity of FBG sensors is proportional to the thermal expansion coefficient of the optical fiber constitutive material – silica, which reduces as the temperature decreases. Approaching cryogenic temperatures, temperature changes lower than a few degrees Kelvin cannot be resolved, for they do not cause an appreciable shift of the wavelength diffracted by a bare FBG sensor (grating elements written on core of the fiber and left recoated).

* Corresponding author. Address: Institute of Technical Physics, Forschungszentrum Karlsruhe, P.O. Box 3640, D-76021 Karlsruhe, Germany. Tel.: +49 7247 82 3827; fax: +49 7247 82 2849.
E-mail address: r-k.ramalingam@itp.fzk.de (R. Rajinikumar).

In order to enhance the sensitivity of FBG sensors at low temperature, it has been proposed [2–5] to embed/recoat the bare FBG sensor with different HTCE polymer of Teflon, PMMA, acrylate and Ormocer materials. But the polymer recoated FBG sensors are not sensitive enough below 77 K and in addition the sensors exhibit non-repeatability characteristic [6]. To improve the sensor sensitivity and its performance characteristics at low temperature, metals are considered for recoating the FBG sensors in present work. This paper reports the evaluation and determination of the design parameters of metal recoated FBG sensors for better performance at low temperature.

2. Theoretical background

The Bragg reflection wavelength λ_B of an FBG is given as [8]

$$\lambda_B = 2 \Lambda n_{eff} \tag{1}$$

where the Bragg grating wavelength, λ_B, is the free space center wavelength of the input light that will be back reflected from the Bragg grating, n_{eff} is the effective refractive index of the fiber core at the free space center wavelength, and Λ is the grating spacing. The FBG is sensitive to strain due to linear expansion affecting the grating period and change in refractive index from the photo-elastic effect. Similarly, it is also sensitive to temperature due to thermal expansion and thermo-optic effect of fiber material. By monitoring the Bragg wavelength shift, $\Delta\lambda_B$ given by Eq. (2), the temperature and strain can be measured [8]:

$$\Delta\lambda_B = 2n\Lambda(\{1 - (n^2/2)[P_{12} - v(P_{11} + P_{12})]\} \\ + [\alpha + (dn/dT)/n]\Delta T \tag{2}$$

where P_{ij} is Pockel coefficient, α is thermal expansion coefficient, v is poisson ratio, ε is strain, and T is temperature.

3. Sensor design

The FBG sensor can be fabricated on a standard single mode fiber. The gratings are written on the core of the fiber after removing the protective sheath by mechanical stripping and removing cladding by chemical wash. The gratings are inscribed on the fiber by passing the laser light through a phase mask [9]. This alters the index of refraction in the photosensitive fiber permanently. After fabricating the grating elements in the fiber, the FBG sensor has to be recoated with selected HTCE metal to enhance the sensor sensitivity and its performance characteristics at low temperature. Therefore, the selection of right material for recoating is foremost important task for the design of high sensitive FBG sensor. Determination of the recoating thickness is the next task of the failure free sensor design. Larger metal recoating thickness affects the measurement speed due to thermal inertia and thinner metal recoating leads to cracks and hence affects to the life time of the sensor. Hence right selection of coating thickness not only improves the sensor life time but also ensures better sensor performance. Fiber losses, birefringence effects can be reduced by proper selection of operating Bragg wavelength and sensor grating length. The accuracy of the measurement and the wavelength division multiplexing (WDM) capability of the FBG sensor can be improved by choosing the sensor grating length carefully. The evaluation and determination of the above discussed sensor design parameters are dealt in detail in the following sections.

3.1. Determination of recoating materials

It is very clear from the above discussions that the materials with HTCE can impart high thermal stress for temperature changes, which in turn can increase the FBG sensor sensitivity. Metals like aluminium, copper, lead and indium are found to have HTCE at cryogenic temperature, which is shown in Fig. 1 [7]. Hence these metals are taken into the consideration.

3.2. Determination of recoating technology

The recoating technology should be rightly selected for coating the fiber with required metals and for required coating thicknesses. Many technologies like dipping, casting, physical vapour deposition (PVD) and chemical vapour deposition (CVD) are available for the metal coating of a bare fiber. Selection of an appropriate method is influenced by the parameters such as process temperature and the thickness of the coating material. The process temperature should be lower than the melting point of the bare fiber as an increased process temperature may damage the sensing elements in FBG. The dipping process cannot be used, as the sensor requires uniform coating throughout the sensing element. Dipping process does not guarantee a uniform coating thickness and the formation
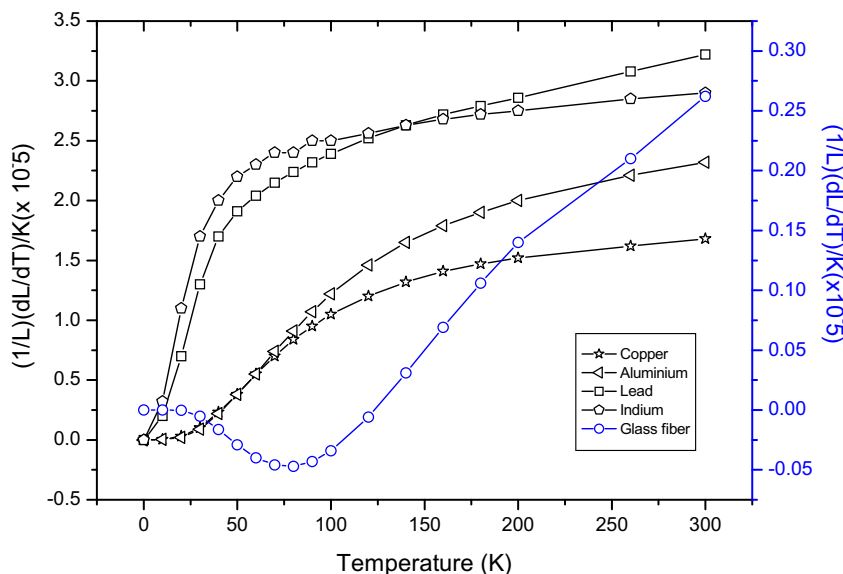

Fig. 1. Thermal expansion coefficient of materials [6].

Lame formula for the stress components at radius r in a circular thick walled tube subjected to internal pressure p_i and external pressure p_e

↓

Stress-strain in cylindrical co ordinate
$$\varepsilon_0 = -\overline{\alpha}\Delta T(1+v) + \frac{1-v^2}{E}\left(\sigma_\theta - \frac{v}{1-v}\sigma_r\right)$$

↓

Radial displacement, $u = r\,\varepsilon_0$

↓

Radial displacement "u_{01}" of the boundary of glass fiber and the radial displacement "u_{11}"of the inner boundary of primary coating.

↓

Radial displacement "u_{12}" of the outer boundary of primary coating and the radial displacement "u_{22}" of the inner boundary of secondary coating

↓

Conditions of the compatibilities of displacements
$u_{01} = u_{11}$
$u_{12} = u_{22}$

↓

Calculated P_1 and P_2 | Give, E_0, E_1, E_2 – Young's Modulus v_0, v_1, v_2 – Poisson's ratio r_0, r_1, r_2 - Radius of fiber and coatings

↓

Radial stress, tangential stress and axial stress in the primary coating and secondary coating can be found by using Lame formula.
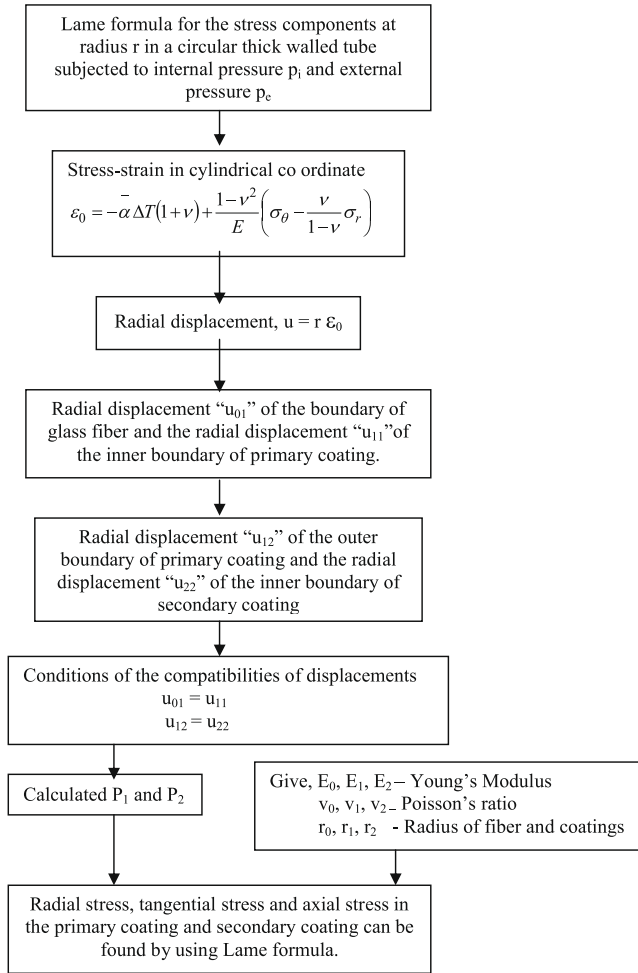
Fig. 2. Flow chart for stress calculations.

of bubbles in the coating layer during the process will also affect the sensor operation. Casting gives higher thermal stresses but allows for a virtually limitless amount of material to be deposited as

a coating. Furthermore, casting cannot be used with metal having a melting point higher than about 700 °C, as this would cause the destruction of the FBG. PVD also produces appreciable thermal stresses. Consequently, electro-deposition is the best suited technique for depositing the metal onto the fiber, as it can be performed at room temperature, thus avoiding thermal stresses, and it allows for the deposition of a large quantity of metals. But fiber is an insulating material and hence metals cannot be deposited directly on the sensor using electro-deposition method. Therefore FBG sensor is recoated by aluminium primary layer and metal secondary layer. Aluminum can be used as the intermediate layer. It may be applied easily to the glass fiber by using Al vaporization technique. This aluminum layer will act like a conductive layer for the electro-deposition of the desired metals.

3.3. Determination of recoating thickness

The thickness of the recoating determines the magnitude of thermal stress acting on the metal recoated FBG sensor. Hence the knowledge of stresses acting in the bare fiber and in the recoating can help in the right determination of recoating thicknesses. The induced stress due to the primary coating layer and the secondary coating layer is calculated by analyzing a simple theoretical model of the dual layer metal coated FBG sensors (DMCFBG). This model is developed by adopting the infinite circular thin walled hollow cylinder model with support of Lame's formula and basic stress-strain relationship [10]. Fig. 2 shows the flow diagram of the analysis which is self sufficient to explain the various steps in the model.

Figs. 3 and 4 show the radial, tangential, and the axial stress distributed in the primary coating layer and the secondary coating layer of the metal recoated Fiber Bragg Grating sensor are calculated for various thicknesses. The superscripts a, b, c and d in the following figures denote the stresses at the inner boundary of the primary coating layer, outer boundary of the primary coating layer, inner boundary of the secondary coating layer and outer boundary of the secondary coating layer, respectively. From Fig. 3, it is seen that the increase in the primary coating thickness increases the stress developed in the primary coating and as the thickness increases more than 125 μm, the increase in the stress rate is very less. Hence the thickness for the primary coating can be chosen as 125 μm. For secondary coating, the thickness of 625 μm can
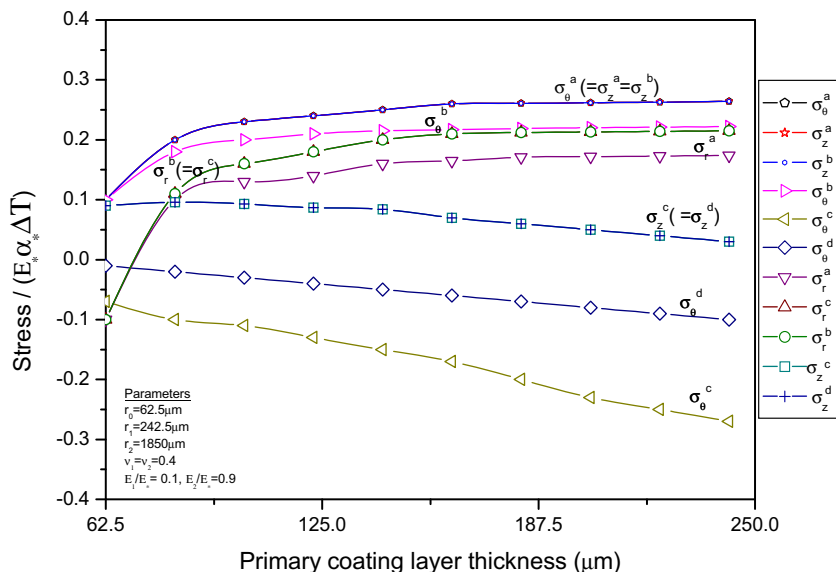

Parameters
r_0=62.5μm
r_1=242.5μm
r_2=1850μm
v_1=v_2=0.4
$E_1/E_* = 0.1$, $E_2/E_* = 0.9$

Fig. 3. Effect of thickness of the primary coating layer on the thermal stresses.

be chosen, after which the stress induced is very small and nearly get saturated. Hence choosing the thickness more than 625 μm is merely going to affect the measurement speed and make the sensor bulky.

3.4. Determination of grating length

Grating length of the FBG sensors can affect the full width half maximum (FWHM) of the back reflected light signal, the temperature, the photo-elastic and the thermo-optic coefficients. The accuracy of the measurement, sensitivity of the sensors and the multiplexing capability of the sensors are the function of the above mentioned parameters. Hence it is essential to study the effect of grating length with respect to these parameters to determine right grating length of the sensor design.

3.4.1. Effect of full width half maximum with respect to grating length
The full width half maximum (FWHM) signal characteristics of the FBG sensors with grating lengths of 2 mm, 5 mm and 10 mm are theoretically calculated using classical coupled mode equations. The theoretically calculated FWHM [FWHM(C)] for 2 mm, 5 mm and 10 mm grating lengths are found to be 0.34 nm, 0.15 nm and 0.09 nm, respectively. A 2 mm, 5 mm and 10 mm grating length elements are then fabricated with the center wavelength of 1535 nm and the FWHM of those sensors are measured. The measured FWHM [FWHM(M)] is then compared with the theoretically calculated FWHM [FWHM(C)], shown in Fig. 5. From the calculations it is observed that the FWHM of the FBG sensors decreases exponentially with the increase in the grating length.

3.4.2. Effect of photo-elastic coefficient with respect to grating length
The effect of the photo-elastic coefficient with respect to various grating length has also been experimentally tested. In the experimental setup, two ends of an optical fiber with a Bragg grating are fixed on both sides to a fixer. The strain is applied to the optical fiber using a pneumatic controller. The reflected spectra are measured at a pressure equal to the strain of 0.05%. From the
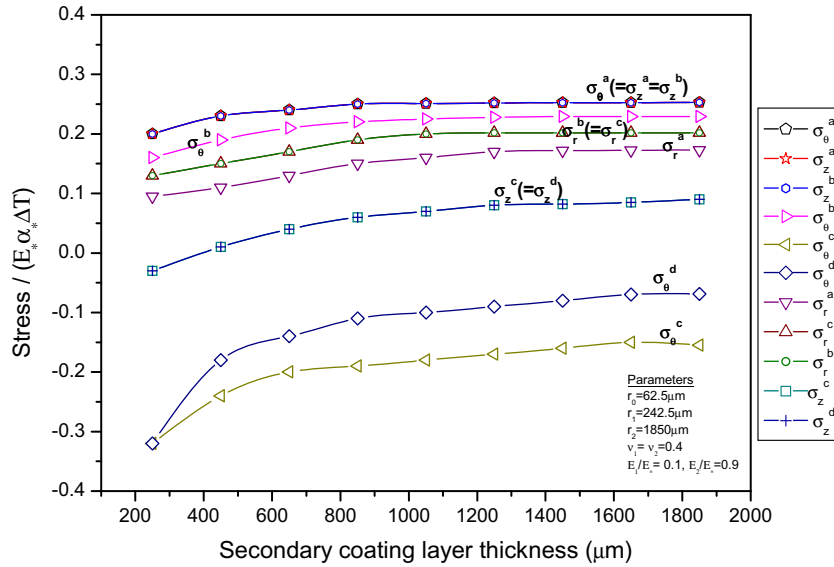

Fig. 4. Effect of coating thickness of the secondary coating layer on the thermal stresses.
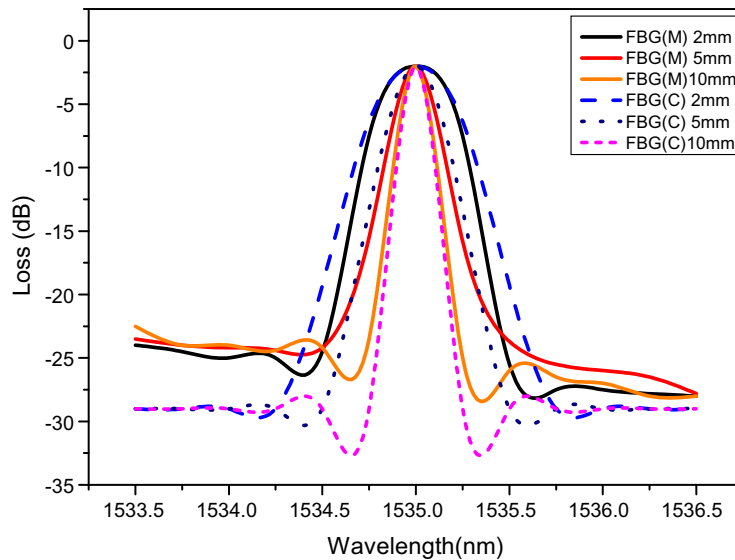

Fig. 5. Calculated and measured reflected wavelength of the 2 mm, 5 mm and 10 mm grating length.

test results, as shown in Fig. 6, it is confirmed that FBG sensors have the same photo-elastic constants regardless of the grating length of the FBG sensor.

3.4.3. Effect of thermo-optic coefficient with respect to grating length

The thermo-optic coefficient can be calculated through the measurement of TEC (thermal expansion coefficient) of an optical fiber, temperature change, and wavelength change. Changes in wavelength and temperature are measured simultaneously from 30 K to 300 K with the temperature interval of 10 K at lower temperature range and 40 K at higher temperature range. In this study, the CTE of an optical fiber is inferred from the material handbook [11]. The calculated thermo-optic coefficient is shown in Fig. 7. From room temperature down to 30 K, the thermo-optic coefficient varies linearly with temperature. This tendency is the same regardless of the grating lengths.

3.4.4. Effect of temperature with respect to grating length

To investigate the signal characteristics of FBG sensors influenced by the temperature, the FBG sensors with different grating lengths of 2 mm, 5 mm and 10 mm are used. Fig. 8 shows the signal changes of the reflected spectra very well. During the cool down, the peak signals are split because of the birefringence induced by the thermal stress developed in the FBG sensor. As the grating length decreases, the birefringence also decreases. The signal of an FBG sensor with a grating length of 2 mm shows no splitting while those of FBG sensors with grating lengths of 5 mm and 10 mm shows split as temperature decreases. Also, it is evident that the peak split of 10 mm is relatively much higher than that of 5 mm. Hence the length of the grating element for high accurate measurement has to be 2 mm. If the application requires several FBG sensors that have to be multiplexed, then grating length with 10 mm can be chosen which has the narrow spectral width
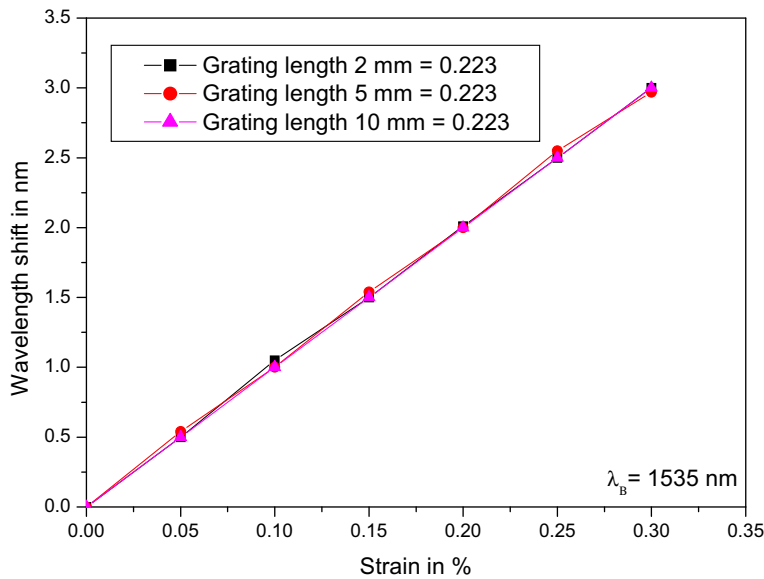

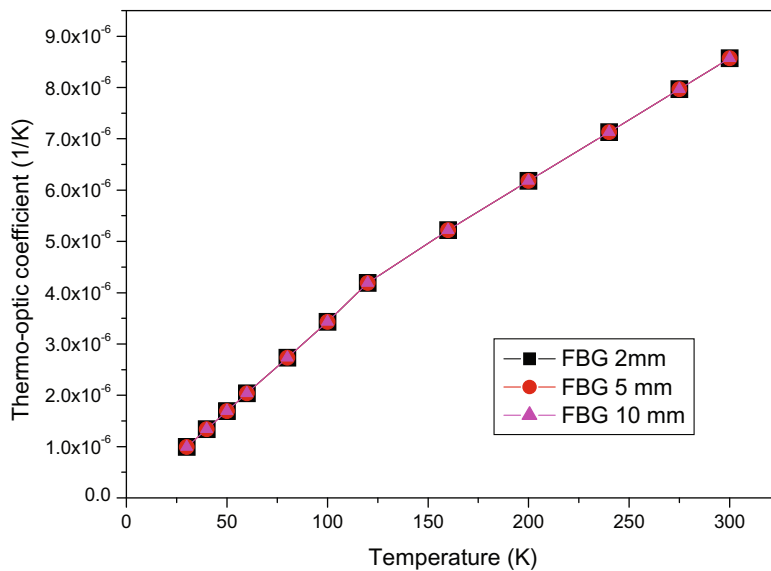**Fig. 6.** Effect of various grating length on the photo-elastic constant of the FBG sensors.

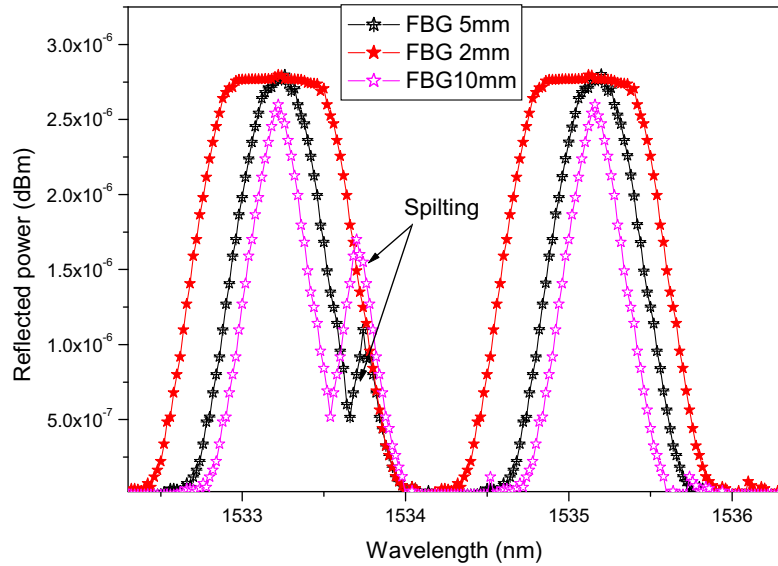**Fig. 7.** Thermo-optic coefficients with respect to temperature change.

Fig. 8. Splitting of FBG spectra during cooling down of various grating lengths.
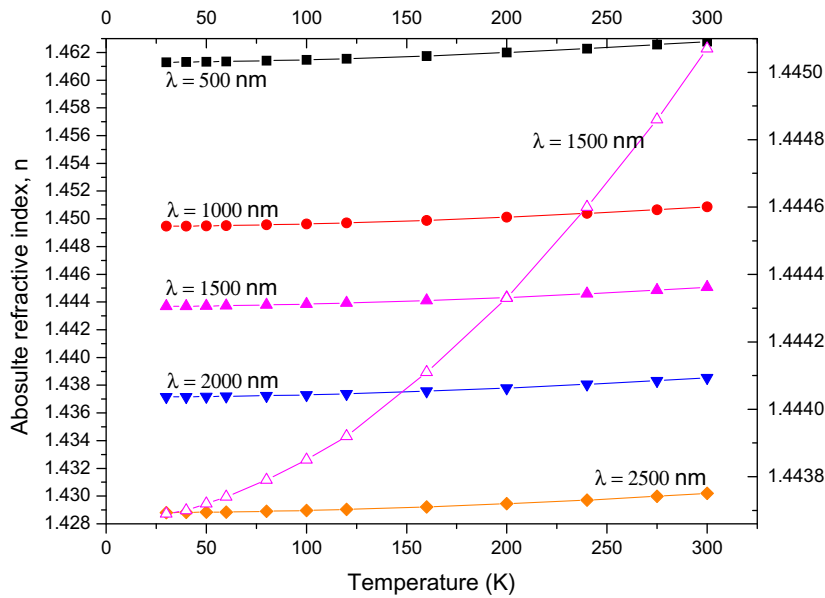

Fig. 9. Change of refractive index of the silica glass fiber with respect to the temperature change.

response. This provides the possibility of multiplexing several sensors in single fiber.

3.5. Determination of Bragg wavelength

Lower the Bragg wavelength, higher is the refractive index. The refractive index can also increase the sensitivity of the FBG sensors. It is expressed as a function of wavelength and temperature using Sellmeier model [12]. From Fig. 9, it is inferred that the refractive index of the silica glass fiber decreases with respect to the wavelength change. Also, it is observed that the change in the refractive index with respect to the temperature is negligible, in other words, it can be assumed to be constant. From Fig. 9, the designer can be lead to choose the Bragg wavelength of 500 nm which could increase the sensitivity. But based on Fig. 10 it can be seen that the dispersion and the losses are high for this wavelength. For temperature change, the dispersion is more or less constant for fixed wavelength. At shorter wavelengths, the loss increases due to Ray-

leigh scattering. At longer wavelengths, it increases due to infrared photon absorption. The thermo-optic coefficient changes with respect to wavelength and temperature changes are shown in Fig. 11. It can be seen that the thermo-optic coefficient remains more or less constant for fixed temperature with varying wavelength, but varies linearly with change in temperature for fixed wavelength. From the above discussion, the Bragg wavelength can be determined to be around 1550 nm or 850 nm, where the dispersion and losses are low when compare to other wavelengths.

4. Conclusion

Proper determination of the design parameters is the key for designing high sensitive and better performance FBG sensor for measuring cryogenic temperature or stresses in superconducting device. The present analysis shows a dual metal coated FBG sensors with primary and secondary layer thickness of around 125 mm and 625 mm, respectively, give better performance for
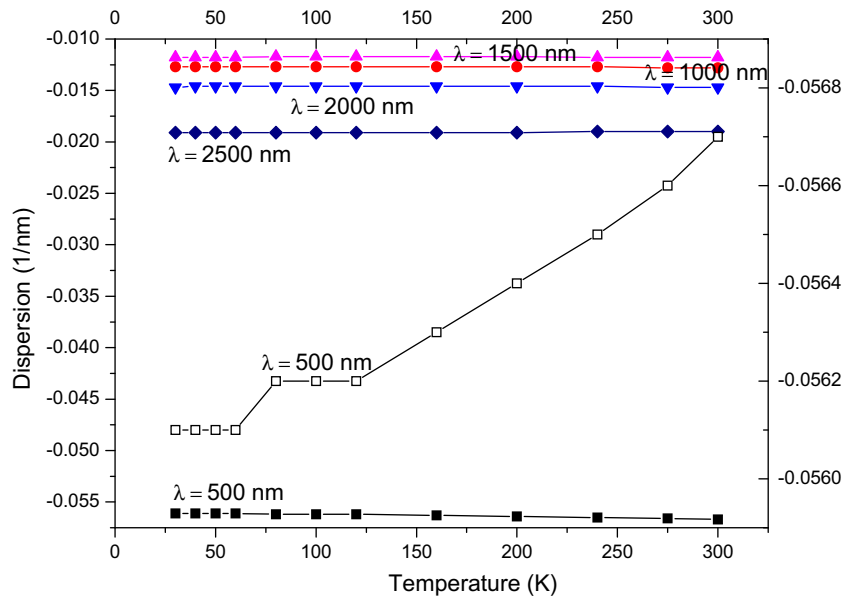
Fig. 10. Change of dispersion with respect to change in temperature at fixed wavelength.
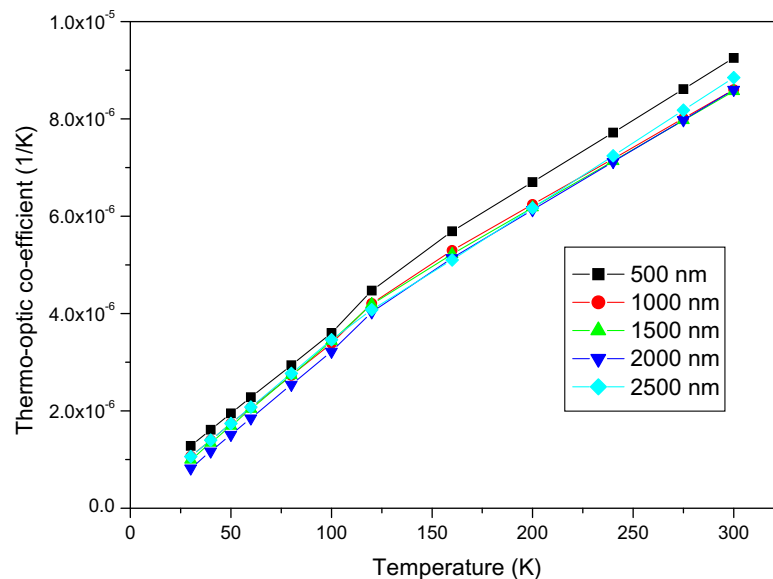

Fig. 11. Thermo-optic coefficient change with respect to temperature change.

the sensor. In addition, the grating period and the grating length of 1500 nm and 2 mm, respectively, give improved accuracy in measurement. The FBG sensor for above mentioned specification is fabricated and tested successfully [1]. The FBG sensors with these designed parameters could be used to measure the thermodynamic parameter distribution inside the superconducting devices. Application of the fibers in magnet devices is expected to be possible either during the CICC assembling process into this structure or during the magnet winding process to the conductor layers.

References

[1] Rajinikumar R, Suesser M, Narayankhedkar KG, Krieg G, Atrey MD. Performance evaluation of metallic coated Fiber Bragg Grating Sensors for sensing cryogenic temperature. Cryogenics 2008;48:142–7.

[2] Mizunami T, Tateata H, Kavashima H. High-sensitivity cryogenic fiber-Bragg-grating temperature sensors using Teflon substrates. Measure Sci Technol 2001;12:914–7.

[3] Li XC, Prinz F, Seim J. Thermal behavior of metal embedded fiber Bragg grating sensor. Smart Mater Struct 2001;10.

[4] Albin S, Fu W, Zheng J, Lavarias AC, Albin J. A cryogenic temperature sensor using fiber Bragg grating. In: Proceedings of ICEC17: cryogenics, section 16. Bournemouth (UK); 1998. p. 695–8.

[5] Rajinikumar R, Nyilas A, Süsser M, Weiss KP, Narayankhedkar KG, Krieg G. Fiber bragg gratings for sensing temperature and stress in super-conducting coils. IEEE Transaction of Applied Superconductivity 2006;16(2) [June].

[6] Rajinikumar R, Nyilas A, Süsser M, Narayankhedkar KG. Investigation of fiber Bragg grating sensors with different coating materials for high sensitivity. In: Proceedings of international cryogenic engineering conference 2006 ICEC 21, Prague. p. 467–70.

[7] Johnson VJ. Properties of materials at low temperature (phase 1). Pergamon Press; 1961.

[8] Othonos A, Kalli K. Fiber Bragg gratings – fundamentals and application in telecommunications and sensing. Artech House Optoelectronics Library; 1999.

[9] Raman Kashyap. Fiber Bragg Gratings. Academic Press; 1999.

[10] Timoshenko SP, Goodier JN. Theory of elasticity. 3rd ed. New York (NY, USA): McGraw-Hill; 1970.

[11] Richard PR, Alan FC. Materials at low temperatures. American Society for Metals; 1983, ISBN 0-87170-146-4.

[12] Wray JH, Neu JT. Refractive index of several glasses as a function of wavelength and temperature. J Opt Soc Am 1969;59(6):774–6.